



Highly Accurate Method for Real-Time Active Power Reserve Estimation for Utility-Scale Photovoltaic Power Plants

Vahan Gevorgian

National Renewable Energy Laboratory

**NREL is a national laboratory of the U.S. Department of Energy
Office of Energy Efficiency & Renewable Energy
Operated by the Alliance for Sustainable Energy, LLC**

This report is available at no cost from the National Renewable Energy Laboratory (NREL) at www.nrel.gov/publications.

Contract No. DE-AC36-08GO28308

**Technical Report
NREL/TP-5D00-73207
February 2019**



Highly Accurate Method for Real-Time Active Power Reserve Estimation for Utility-Scale Photovoltaic Power Plants

Vahan Gevorgian

National Renewable Energy Laboratory

Suggested Citation

Gevorgian, Vahan. 2019. *Highly Accurate Method for Real-Time Active Power Reserve Estimation for Utility-Scale PV Power Plants*. Golden, CO: National Renewable Energy Laboratory. NREL/TP-5D00-73207. <https://www.nrel.gov/docs/fy19osti/73207.pdf>.

**NREL is a national laboratory of the U.S. Department of Energy
Office of Energy Efficiency & Renewable Energy
Operated by the Alliance for Sustainable Energy, LLC**

This report is available at no cost from the National Renewable Energy Laboratory (NREL) at www.nrel.gov/publications.

Contract No. DE-AC36-08GO28308

Technical Report
NREL/TP-5D00-73207
February 2019

National Renewable Energy Laboratory
15013 Denver West Parkway
Golden, CO 80401
303-275-3000 • www.nrel.gov

NOTICE

This work was authored by the National Renewable Energy Laboratory, operated by Alliance for Sustainable Energy, LLC, for the U.S. Department of Energy (DOE) under Contract No. DE-AC36-08GO28308. Funding provided by U.S. Department of Energy Office of Energy Efficiency and Renewable Energy Solar Energy Technologies Office. The views expressed herein do not necessarily represent the views of the DOE or the U.S. Government.

This report is available at no cost from the National Renewable Energy Laboratory (NREL) at www.nrel.gov/publications.

U.S. Department of Energy (DOE) reports produced after 1991 and a growing number of pre-1991 documents are available free via www.OSTI.gov.

Cover Photos by Dennis Schroeder: (clockwise, left to right) NREL 51934, NREL 45897, NREL 42160, NREL 45891, NREL 48097, NREL 46526.

NREL prints on paper that contains recycled content.

Preface

This paper applies a robust technique for determining the available power from a curtailed utility-scale photovoltaic (PV) power plant. The proposed technique does not require deploying any additional equipment or sensors and is based only on the addition of new control logic to the existing power plant controller. Also, the proposed method is universally applicable to PV plants with any type of smart inverters and PV modules. Accurate determination of available power is important for using curtailed PV generation as a resource for various types of active power controls, such as spinning reserves and primary and secondary frequency control. For PV plants to be able to maintain the desired regulation range, the plant controller must be able to estimate the available aggregate peak power that all the plant's inverters can produce at any point in time and ensure that the control error stays within the tolerance band at all times. In this paper, we explore a highly accurate control method that uses dedicated inverters within the plant as reference units and evaluates the available aggregate peak power for the whole plant under different cloud variability conditions.

Acknowledgments

The author thanks Guohui Yuan and Anastasios Golnas of the U.S. Department of Energy's Solar Energy Technologies Office for their continuous support of this project. Thank you also Mahesh Morjaria and other members of First Solar team.

List of Acronyms

MPP

MPPE

MPPT

PV

Maximum power point

Maximum power point estimation

Maximum power point tracking

Photovoltaic

Table of Contents

Introduction	1
1 Proposed Method	4
2 Data	7
3 Statistical Analysis Methods	9
4 Placement of Reference Inverters.....	10
5 Correlation of Measured and Estimated MPPT Power for Entire PV Plant.....	11
6 Maximum Power Estimation Error Statistics	17
7 Conclusions	21
8 Future Plans	22
References	23

List of Figures

Figure 1. Example of inaccurate maximum power estimation	3
Figure 2. Example of maximum power estimation using a single reference inverter.....	3
Figure 3. Large PV power plants under clear-sky conditions—only one reference MPP inverter is used...	5
Figure 4. Large PV power plant divided into control zones during cloud conditions	5
Figure 5. Snapshot of measured AC power output variability across the PV plant.....	7
Figure 6. Four variability cases used in the analysis.....	8
Figure 7. Minimum curtailment level as a function of the number of reference inverters	8
Figure 8. Assigning different numbers of reference inverters within the array footprint. (Red dots represent sections of the array connected to reference MPPT inverters.).....	10
Figure 9. Calculating the error in estimated maximum power.....	10
Figure 10. Clear-sky case: a high level of accuracy in maximum power evaluation can be achieved even with a single reference inverter, and it can be further improved with four inverters. (Blue: measured total plant power when operating in MPPT mode; red: estimated total plant power for different numbers of reference inverters. The red cannot be distinguished from blue because of high accuracy of estimation.).....	11
Figure 12. Improving the accuracy of maximum power evaluation by using a larger number of reference inverters: moderate variability case. (Blue: measured total plant power when operating in MPPT mode; red: estimated total plant power for different numbers of reference inverters.)	12
Figure 13. Improving the correlation between measured and evaluated maximum power by using a larger number of reference inverters: moderate variability case.....	13
Figure 14. Improving measured total plant power when operating in MPPT mode; red: estimated total plant power for different numbers of reference inverters.).....	13
Figure 15. Improving the correlation between measured and evaluated maximum power by using a larger number of reference inverters: intense variability case	14
Figure 16. Improving the accuracy of maximum power evaluation by using a larger number of reference inverters: extreme variability case. (Blue: measured total plant power when operating in MPPT mode; red: estimated total plant power for different numbers of reference inverters.)	14
Figure 17. Improving the correlation between measured and evaluated maximum power by using a larger number of reference inverters: extreme variability case.....	15
Figure 18. Improving accuracy for an extreme variability case. (Blue: measured total plant power when operating in MPPT mode; red: estimated total plant power for different numbers of reference inverters)	16
Figure 19. Reduction of control error with increasing numbers of reference inverters. (A: moderate variability case; B: extreme variability case.).....	17
Figure 20. Mean error and standard deviation of error	19
Figure 21. Min and max estimation error	19
Figure 22. Skewness and kurtosis of error distribution.....	20
Figure 23. Correlation coefficients for all variability cases.....	20
Figure 24. Aerial photo of First Solar PV plant at the National Renewable Energy Laboratory’s National Wind Technology Center	21
Figure 25. Typical MW-scale PV inverter efficiencies	22

List of Tables

Table 1. Mean Peak Power Evaluation Error (% of Plant Rated Power).....	18
Table 2. Standard Deviation of Peak Power Evaluation Error (% of Plant Rated Power).....	18
Table 3. Maximum Positive Peak Power Evaluation Error (% of Plant Rated Power)	18
Table 4. Maximum Negative Peak Power Evaluation Error (% of Plant Rated Power).....	18
Table 5. Skewness of Peak Power Evaluation Error Distribution (% of Plant Rated Power).....	19
Table 6. Kurtosis of Peak Power Evaluation Error Distribution (% of Plant Rated Power).....	19
Table 7. Correlation Coefficients Between Actual and Estimated Available Power for All Variability Cases.....	20

Introduction

All over the world, system operators and utilities are continually adapting their grid codes, interconnection requirements, operational practices, and market mechanisms to make the integration of shares of fast-growing variable renewable generation both reliable and economic [1]. As power systems continue to evolve, the Federal Energy Regulatory Commission (FERC) noted that there is a growing need for a refined understanding of the services necessary to maintain a reliable and efficient system. In orders 755 and 784, FERC required improving the mechanisms by which frequency regulation services are procured and enabling compensation by fast-response resources such as energy storage. In addition, FERC recently issued a notice of proposed rulemaking to enable the aggregation of distributed storage and distributed generation [2]. The North American Electric Reliability Corporation's (NERC) Integration of Variable Generation Task Force made several recommendations for requirements for variable generators (including solar) to provide their share of grid support, including active power control (APC) capabilities [3], [4]. Similar requirements for renewable energy plants have been introduced in Europe at both the transmission and distribution levels [5], [6]. In 2018, FERC Order 842 amended the pro forma interconnection agreements to include certain operating requirements, including maximum droop and dead band parameters, and sustained response provisions [7].

NERC's BAL-003-1 standard on frequency response establishes target contingency protection criteria for each North American interconnection and individual balancing authorities (BAs) within interconnections [8]. BAs are required to meet the minimum frequency response obligation (FRO), so the generating resources that are operated in a mode and range to meet the FRO need to have adequate headroom to respond to frequency transients and load-frequency control set points. Although establishing such headroom is not a problem for the conventional fleet, the varying nature of solar and wind generation makes it challenging to set and maintain adequate headroom by these varying resources.

In general, all system operators have processes and procedures in place to ensure grid reliability through monitoring market participant operation. For example, provisions of the California Independent System Operator (CAISO) tariff [9] set penalties for deviations from dispatch and regulation capacity for market participants that fail to perform in compliance. The permitted area of variation for performance requirements of resources used for various purposes is provided in the CAISO tariff [9]. The tolerance band is expressed in terms of energy (MWh) for generating units and imports from external dynamic system resources for each settlement interval and equals the greater of the absolute value calculated using either of the following methods:

1. 5 MW divided by the number of settlement intervals per settlement period
2. 3% of the relevant generating unit's maximum output (P_{\max}), as registered in the master file, divided by the number of settlement intervals per settlement period.

This CAISO tariff and similar requirements from other system operators imply that accurate real-time estimations of available maximum power from the curtailed photovoltaic (PV) plant are important for avoiding excessive penalty payments if utility-scale PV plants become market participants for energy and various reliability services related to active power controls.

A typical modern utility-scale PV power plant is a complex system of large PV arrays and multiple power electronic inverters, and it can contribute to mitigating the impacts on grid stability and reliability through sophisticated, automatic “grid-friendly” controls. To provide active power reserves (or a headroom margin) for up-regulation that can be automatically dispatched as needed, the PV plant needs to operate below its maximum power point (MPP); however, evaluating that MPP in curtailed mode is not a trivial task, especially for large PV power plants during various types of variable conditions caused by clouds. One paper [10] proposed an experimentally validated maximum power point estimation (MPPE) method that operates in real time using irradiance and cell temperature measurements to ensure that sufficient reserve power is available. Another paper [11] proposed an advanced real-time MPPE algorithm by applying curve fitting on voltage and current measurements obtained during inverter operation. Some previously proposed MPPE methods used offline prediction and employed regression analysis or neural networks [12], [13]. These methods seem to be accurate but might require excessive processing power. Others proposed methods for real-time calculation [14]–[16] by making assumptions that reduce the accuracy of the PV model or, in some cases, require knowledge that is not typically available on PV module data sheets [14], [17]. Another important limitation of MPPE methods is that modifications are needed based on inverter types and topologies. For example, in single-stage inverters (no DC/DC conversion), the power reserve capability can be achieved by inverter control modifications [18], [19]. In two-stage systems (inverter and DC/DC converter), however, the DC/DC converter control needs to be modified instead [20]. This makes the use of maximum power estimation for curtailed PV systems challenging and highly dependent on inverter make and topology, types of modules used in PV plants, and accurate knowledge of the inverter and PV module parameters.

The variability of solar PV output in the regulation reserve time frame among various arrays within a large-scale (~50-MW) solar PV plant in the southwestern United States is discussed in [21]. Although the distributions of changes in aggregate power output throughout all timescales considered were clustered around a strong peak at zero, the distributions at all timescales exhibited significant instances of higher magnitude ramps in the tails of the histograms. The results achieved in [21] were very important because the method presented in this paper was also tested using the data from the same PV power plant.

In 2015, a demonstration project was conducted in the U.S. territory of Puerto Rico using a 20-MW grid-connected PV power plant [22]. This plant was controlled to provide different types of reliability services to the island’s grid including various types of active power controls. Testing on this plant provided real data on levels of uncertainty that can be introduced by traditional MPPE methods based on irradiance and temperature measurements as well as inverter I–V characteristics. One example of such uncertainty is shown in Figure 1 during operation when the PV plant was responding to an automatic generation control (AGC) signal sent from the system operator. The AGC system assumed that there was still some available headroom for up-regulation because its evaluation was based on the available plant power value that was communicated by the power plant controller (PPC). The calculated available power is overly optimistic, however, and inverters are not able to produce as much power because they are already operating at the maximum peak power point. Note that the mismatch at lower curtailment level shown in Figure 1 is because of the minimum curtailment limit set by the plant owner for economic reasons.

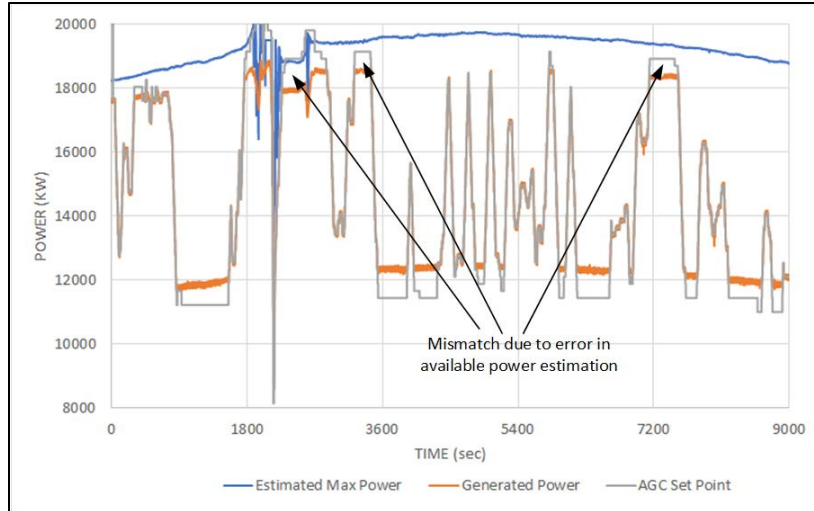


Figure 1. Example of inaccurate maximum power estimation

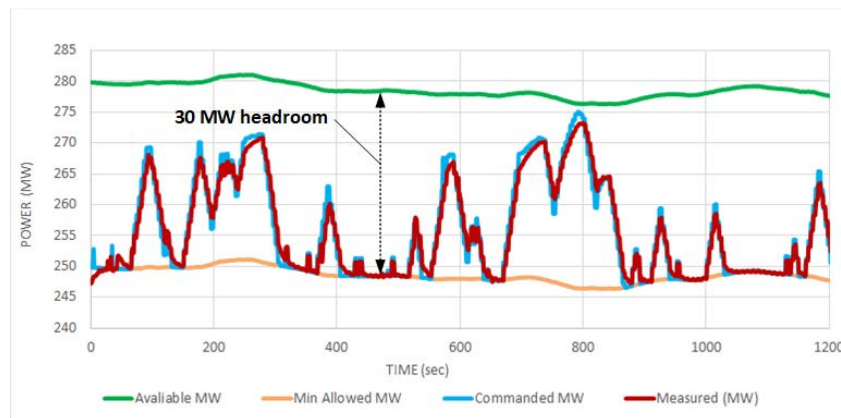


Figure 2. Example of maximum power estimation using a single reference inverter

A different method for estimating the maximum power was used during the demonstration testing of a 300-MW PV power plant in California [1]. In this case, a single 4-MVA inverter was taken from the AGC scheme and was set to operate at the power level determined by its maximum power point tracking (MPPT) algorithm. The measured AC power of this inverter was used as an indicator of available power for the other 79 inverters (80 inverters total), so the plant was able to operate with fixed 30 MW of headroom (Figure 2). This method also has inherent uncertainties because it assumes uniform solar resource conditions across the whole 300-MW plant. Fortunately, cloud conditions were favorable for this method to be acceptable because there was a clear sky above the plant during most of the testing day.

The method proposed in this paper is also based on using dedicated reference inverters within a curtailed PV power plant for estimating the maximum available power; however, it is based on the use of multiple reference inverters to achieve high levels of real-time maximum power estimation under conditions of extreme variability.

1 Proposed Method

For utility-scale PV power plants to be able to maintain the desired regulation range or spinning reserve levels, the plant controller must be able to estimate the available aggregate peak power that all the plant's inverters can produce at any point in time. The available power is normally estimated by an algorithm that considers solar irradiation, the characteristics and temperatures of PV modules I–V , inverter efficiencies, etc.; however, this method has many uncertainties, depends on the availability of accurate system models, and does not account for other factors such as panel soiling because of dust. The proposed method can determine the available peak power of the PV plant and maintain desired reserves with high levels of accuracy without the use of external sensors or devices. The existing plant hardware and controls can perform this task after the addition of the new optimized control algorithm in power plant controller software.

Under clear-sky conditions, a single PV inverter can be used as a reference for the whole plant to determine the available power at any point in time (Figure 3). Under variable-cloud-cover conditions, however, a single-inverter method will not be accurate enough for large PV power plants. Instead, we propose a concept that can accurately allocate reserves for PV power plants by:

- Creating dynamic virtual control zones in the PV plant
- Determining which PV inverter is to serve as a reference by operating at MPP
- Determining the optimal dispatch interval for the reference MPP inverters based on the rate of change of the power in each zone (i.e., indicator of cloud movement)
- Determining the optimized combinations of the curtailment set points for participating inverters in each zone for the maximum aggregate inverter efficiency (or minimum electric losses in the plant) for every control interval.

The idea for such a method is shown in Figure 4. The plant controller allocates virtual dynamic control zones consisting of two or more inverters depending on the cloud conditions over the plant. Then, a single inverter in each virtual group is operated at MPP and is used as a reference for determining the maximum available power for the zone so that appropriate curtailment set points can be sent to all participating inverters within the zone. After a certain time interval, the process is repeated, ensuring accurate reserve allocation by the whole plant and avoiding excessive curtailments.

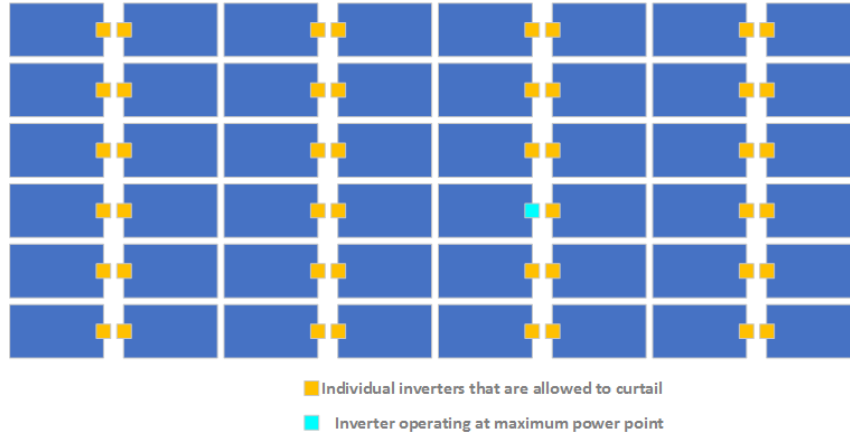


Figure 3. Large PV power plants under clear-sky conditions—only one reference MPP inverter is used



Figure 4. Large PV power plant divided into control zones during cloud conditions

In this report, we use the following abbreviations:

- N_{total} : total number of inverters in the PV power plant
- N_{zones} : number of control zones (the same as the number of reference inverters N_{ref})
- $N_{inv} = \frac{N_{total}}{N_{zones}}$: number of inverters in each control zone
- $P_{total.max}$: total power production of the plant when all inverters are operating at MPP
- $P_{max,i}$: power production of zone i when all inverters in the zone are operating at MPP
- $P_{mppt,i}$: power production by a single inverter operating at MPP in zone i .

The estimated maximum available power from the plant using instantaneous power produced by single MPPT inverters in each zone (blue inverters in Figure 4) is determined as:

$$P_{total.max}^{est} = \sum_{i=1}^{N_{zones}} N_{inv} \cdot P_{mppt,i} \quad (1)$$

Plant curtailment set point as a percentage of estimated maximum available power from the plant is determined as:

$$P_{total}^{set} = (1 - \Delta P) \cdot P_{total.max}^{est} \quad (2)$$

where ΔP (in per units) is a curtailment set point. For example, $\Delta P = 0.1$ means that the plant is expected to operate with 10% active power reserve margin or at 90% of P_{total}^{set} .

Power set points to all individual inverters in zone i that are participating in the curtailment scheme (orange inverters in Figure 4) can then be calculated:

$$P_{inv,i} = P_{mppt,i} \cdot \frac{N_{inv}(1-\Delta P)-1}{N_{inv}-1} \quad (3)$$

Therefore, the power production of zone i can be calculated as:

$$P_{zone,i} = P_{mppt,i} + (N_{inv} - 1) \cdot P_{inv,i} \quad (4)$$

And the total power production of the plant operating with the curtailment set point ΔP is:

$$P_{plant} = \sum_{i=1}^{N_{zones}} P_{zone,i} = [N_{inv}(1 - \Delta P) - 1] \cdot \sum_{i=1}^{N_{zones}} P_{mppt,i} \quad (5)$$

2 Data

In this work, we examined the applicability of the proposed method using solar PV output power data from different arrays in a single utility-scale (~50-MW) PV plant in the western United States. The plant consists of 96 individual inverters, each rated at 0.5 MW. We used 1-s power data from each individual inverter collected from the plant during a period of several months, allowing us to analyze the accuracy of the proposed method under different resource variability scenarios.

A depiction of the geographic layout of the individual 0.5-MW PV arrays is shown in Figure 5. The figure also shows a snapshot of the variability of the measured AC electric power among different sections of the plant. After analyzing many days of measured data, we decided to use plant data sets from four different days characterizing four different variability scenarios: (1) clear sky, (2) moderate variability, (3) intense variability, and (4) extreme variability. One-second time series for each selected variability case is shown in Figure 6A. For comparison, we show the 1-s rate of change of the total plant power (Figure 6B) and the frequency distribution of 1-s power changes (Figure 6C). The extreme variability case shown in Figure 6C had the largest 1-s changes in plant power output during the whole period of observation. The maximum positive and negative 1-s changes in power are +0.6 MW and -0.42 MW, respectively (or +1.25% and -0.87% of the plant's rated power). One observation from Figure 6C is that the distribution of the 1-s power changes for the extreme variability case is nonsymmetric, and the distribution has a longer positive tail. This can be explained by the different up- and down-ramp limit settings in the inverters. When selecting these data sets, care was taken to make sure that the variability in the output was caused by changing solar irradiance conditions only, not trip-off events.

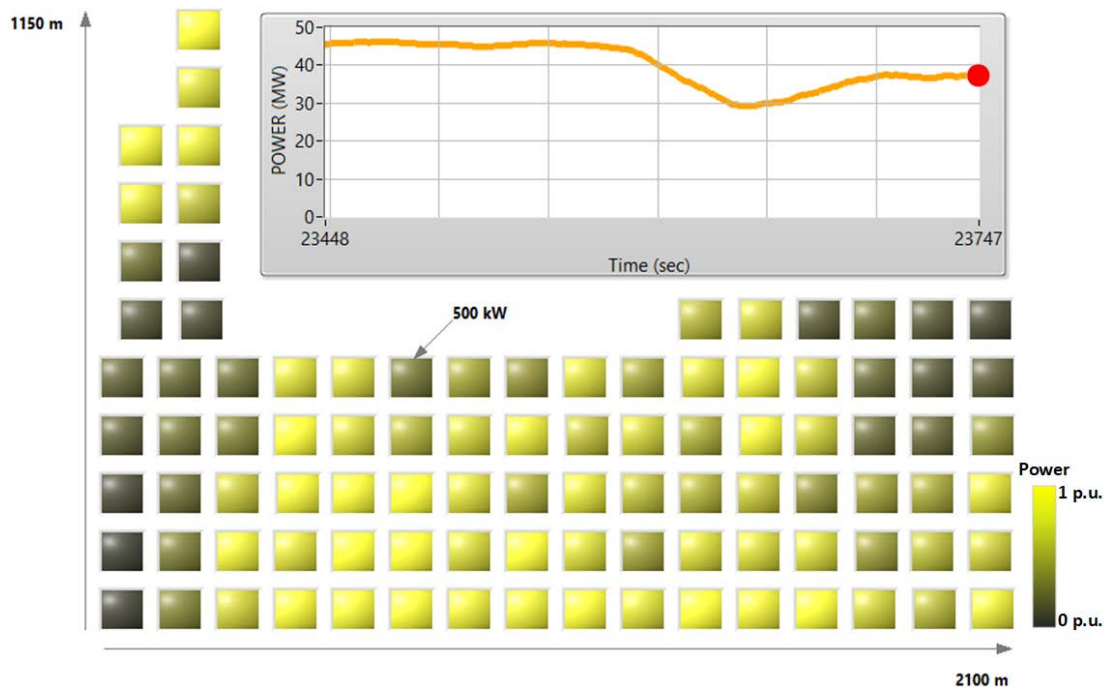


Figure 5. Snapshot of measured AC power output variability across the PV plant

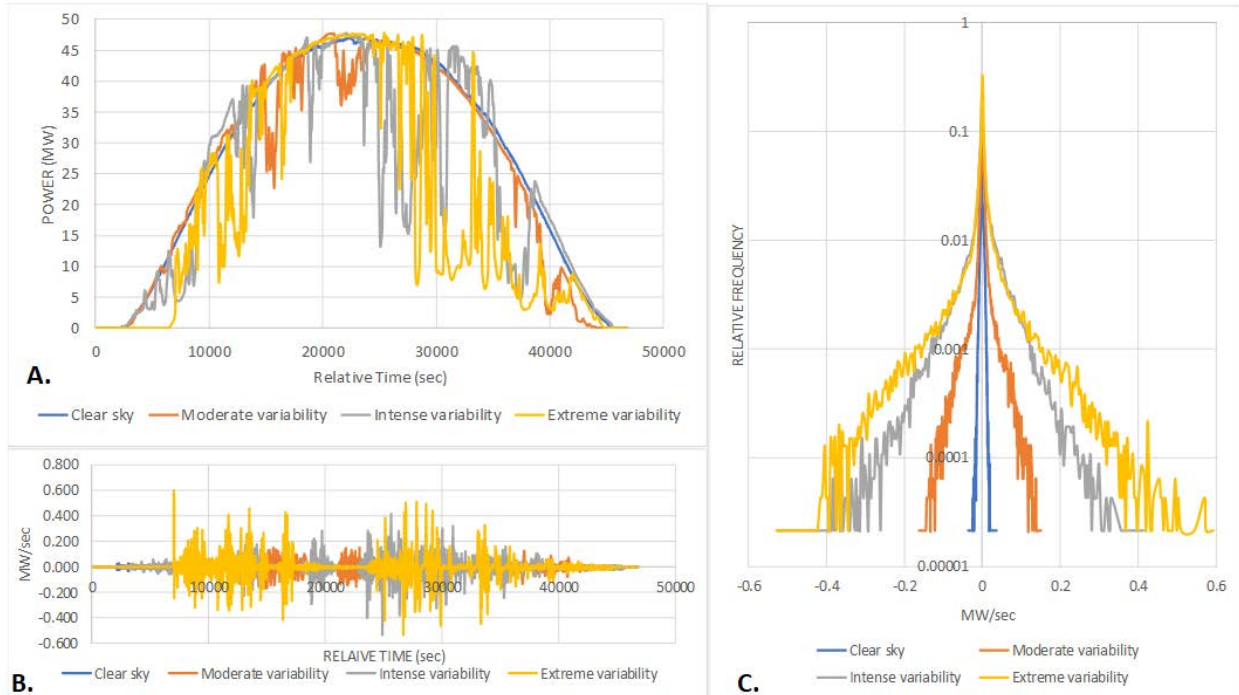


Figure 6. Four variability cases used in the analysis

Note that the proposed method is expected to provide an accurate estimation of available peak power only for curtailment levels that are above a certain minimum curtailment threshold. This threshold is determined by the number of inverters from equations (1)–(5) as follows. For example, for the case of $N_{ref} = 48$, there are 48 inverters operating at MPPT, leaving the remaining 48 inverters available for curtailment. Therefore, the plant can be curtailed only down to 50% of available power for $N_{ref} = 48$. The calculated minimum curtailment for different numbers of reference inverters is shown in Figure 7. For smaller numbers of reference inverters, the plant can be curtailed to much lower levels, as shown in Figure 7.

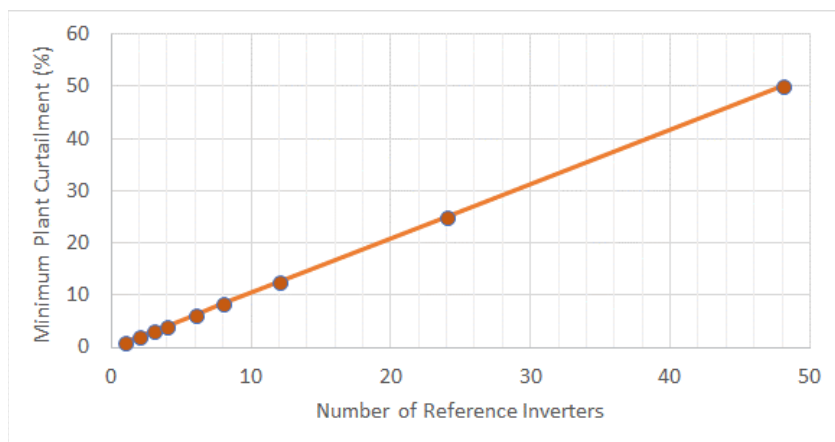


Figure 7. Minimum curtailment level as a function of the number of reference inverters

3 Statistical Analysis Methods

Some of the statistical background that was used in the 1-s maximum power evaluation analysis is described in this section using [23], [24], and [25]. We used a histogram as a graphical method to display the shape of the distribution for control errors for maximum evaluated power data. The class intervals, or bin widths, were determined using the square-root method, which calculates the number of bins as a square root of the number of data points in the sample [26] ($N_{bins} = \sqrt{N_{data}}$). Only daytime production hours (6 a.m.–7 p.m.) were used in the analysis, totaling $N_{data} = 46,800$ (equal to the number of seconds from 6 a.m.–7 p.m.). The bin widths were then calculated directly from the maximum and minimum values in the data. For data sets with a large number of points, a histogram essentially resembles continuous frequency distributions because of the large number of bins.

In addition to the histogram analysis, standard deviation, and mean, we applied two more statistical measures to the characterization of the error distributions: skewness and kurtosis. Skewness is a measure of symmetry (or, more precisely, the lack of symmetry) for a given data set, and it is defined as:

$$\gamma = \frac{\sum_{i=1}^N (x_i - \mu)^3}{(N-1)\sigma^3} \quad (6)$$

where γ is the skewness, μ is the mean, σ is the standard deviation, and N is the number of data points in the set. The skewness for a normal distribution is zero, and any symmetric data set should have a skewness near zero.

Kurtosis is the degree of peakedness of a distribution. It is a measure of the magnitude of the peak of the distribution or, conversely, how fat-tailed the distribution is. It is defined as:

$$K = \frac{\sum_{i=1}^N (x_i - \mu)^4}{(N-1)\sigma^4} - 3 \quad (7)$$

In this definition of kurtosis, data sets with a higher value of kurtosis tend to have a distinct peak near the mean and decline rather rapidly.

Correlation coefficients are used in the statistics to measure the strength of the relationship between two data sets. In this analysis, we used the Spearman's rank correlation coefficient, commonly used to measure the degree of association between two variables:

$$R = 1 - \frac{6 \sum d_i^2}{n(n^2-1)} \quad (8)$$

where R is the Spearman's rank correlation coefficient, x and y are elements of data sets, d is the difference between the ranks of the corresponding variables, and n is the number of observations.

It is general practice in statistical analysis of acquired time series data to remove the outliers (data points that lie an abnormal distance from other values in a sample). This is usually accomplished by removing values that are greater than a certain percentile value (for example, the 99th percentile). In this analysis, we did not perform any outlier screening in the ramp rate data. The reason for this is that extreme ramp rate events that lie in the tails of the observed distribution are of significant interest in the context of this work and will have an impact on the accuracy of the proposed maximum power evaluation method.

4 Placement of Reference Inverters

The total plant 1-s production data and data from 96 individual inverters for four variability cases were used to evaluate the ability of the proposed method to accurately predict the maximum available power from the entire plant for different numbers of reference inverters. The following numbers of control zones with a single reference inverter in each zone were used in the analysis of the number of reference inverters: $N = 1, 2, 3, 4, 6, 8, 12, 24, 48$. A simple algorithm was developed to select the locations of the reference inverters using an equidistant approach. The selected locations of the reference inverters for each case are shown in Figure 8, where the red dots represent single 0.5-MW arrays with their inverters operating in MPPT mode (reference inverters). For example, for $N = 1$, there is only one reference inverter and the algorithm choose it to be in the center of the plant. For $N = 2$, there are two reference inverters placed in two sections of the plant, etc. For $N = 48$, there are 48 reference inverters out of the total 96 inverters. In this case, the algorithm breaks the whole plant into pairs of individual inverters where one inverter operates in MPPT reference mode.

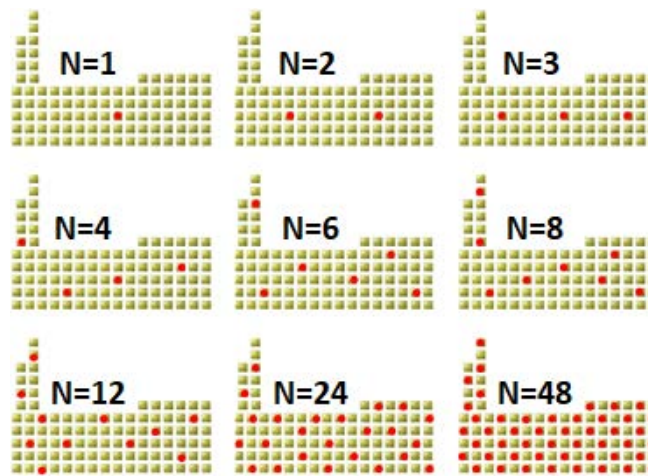


Figure 8. Assigning different numbers of reference inverters within the array footprint. (Red dots represent sections of the array connected to reference MPPT inverters.)

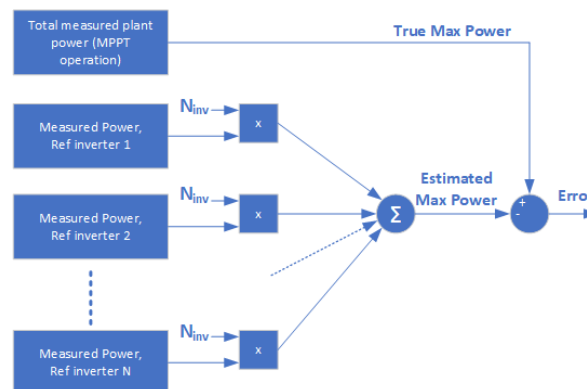


Figure 9. Calculating the error in estimated maximum power

The estimated maximum power of the plant can be calculated using Eq. (1) for any number of reference MPPT inverters. Then, the estimation error can be evaluated as shown in Figure 9.

5 Correlation of Measured and Estimated MPPT Power for Entire PV Plant

Correlation measures the linear dependence between two variables, and correlation values fall within the range from -1 to 1. A value of 1 indicates that one variable is a positive linear function of the other, a value of -1 means that one variable is a negative linear function of the other, and 0 indicates a lack of correlation entirely. In this section, we use the Spearman's rank correlation coefficient (Eq. 8) to measure the linear correlation between measured 1-s total plant power operating in MPPT mode with estimated maximum available peak power from the plant operating in curtailed mode at different numbers of reference inverters with locations shown in Figure 8. The Spearman's rank correlation method does not carry any assumptions about the frequency distribution of the data sets, allowing us to determine whether two ranked variables covary (i.e., as one variable increases or decreases, the other variable tends to follow). Further statistical analysis of the evaluated power will be performed in Section 7.

First, we analyze the ability of the proposed method to estimate the available peak plant power for a clear-sky case (as defined in Figure 6). In this case, even with one reference inverter, there is a very strong correlation between measured and estimated 1-s peak power data, as shown in Figure 10 (upper graphs). This observation is consistent with results of the test conducted on a 300-MW PV plant as described in [1]. With increasing numbers of reference inverters, the correlation becomes even stronger. For example, with only four reference inverters, the correlation is basically ideal as shown in Figure 10 (lower graphs).

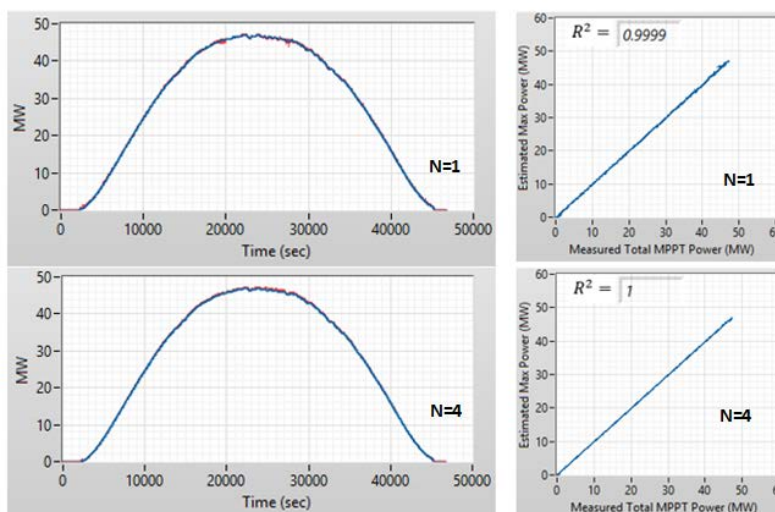


Figure 10. Clear-sky case: a high level of accuracy in maximum power evaluation can be achieved even with a single reference inverter, and it can be further improved with four inverters. (Blue: measured total plant power when operating in MPPT mode; red: estimated total plant power for different numbers of reference inverters. The red cannot be distinguished from blue because of high accuracy of estimation.)

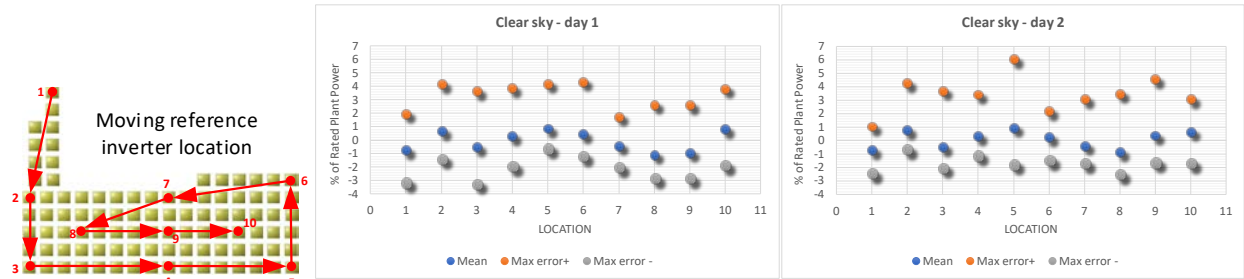


Figure 11. Maximum power estimation error for different reference inverter locations (clear-sky case)

Changing the location of reference inverter in clear-sky case has very small impact on mean estimation error (blue dots) as shown in Figure 11 for two consecutive clear-sky days.

These observations suggest that even with a low number of reference inverters, the proposed method can track the true available power with a high degree of correlation on a second-by-second basis for clear-sky conditions. This picture changes drastically for cases with variability caused by cloud movements, as further described using results shown in Figure 12–Figure 18 for three different variability conditions.

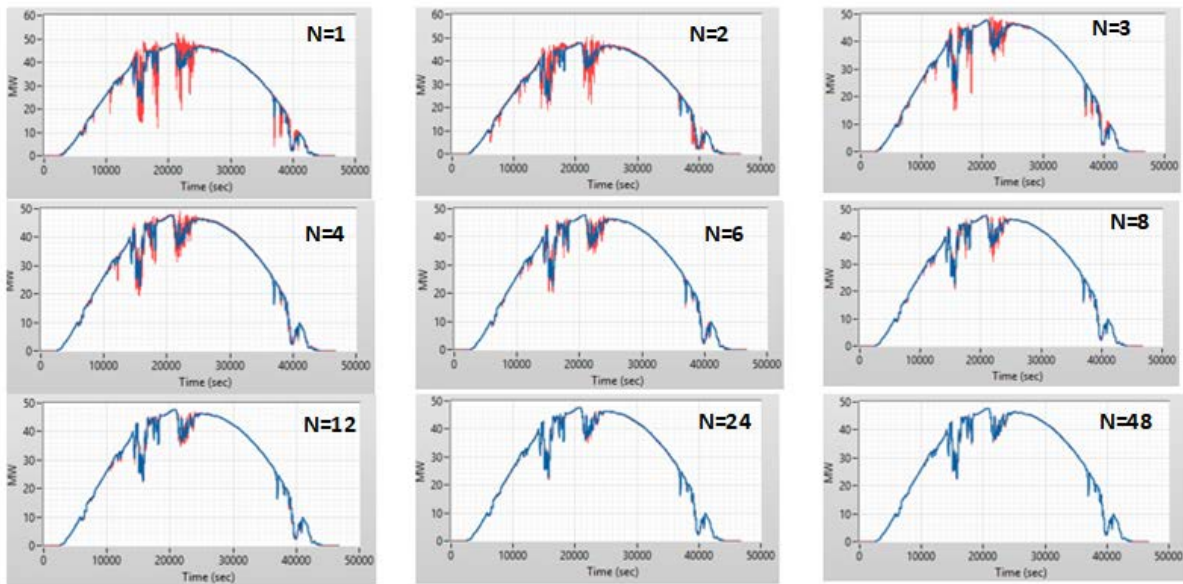


Figure 12. Improving the accuracy of maximum power evaluation by using a larger number of reference inverters: moderate variability case. (Blue: measured total plant power when operating in MPPT mode; red: estimated total plant power for different numbers of reference inverters.)

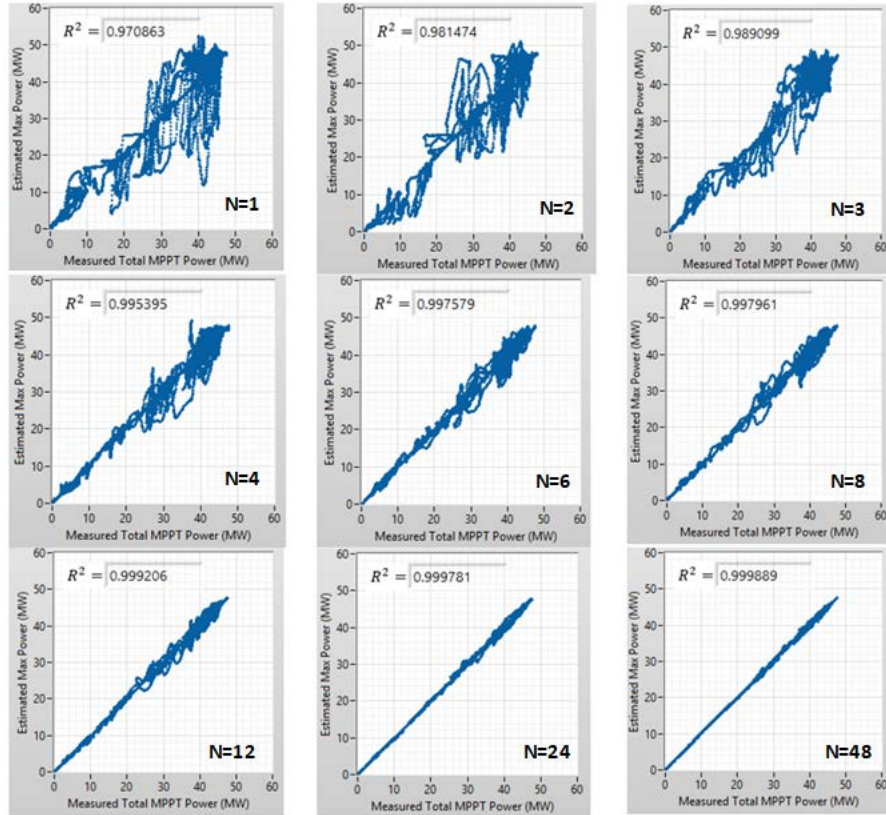


Figure 13. Improving the correlation between measured and evaluated maximum power by using a larger number of reference inverters: moderate variability case

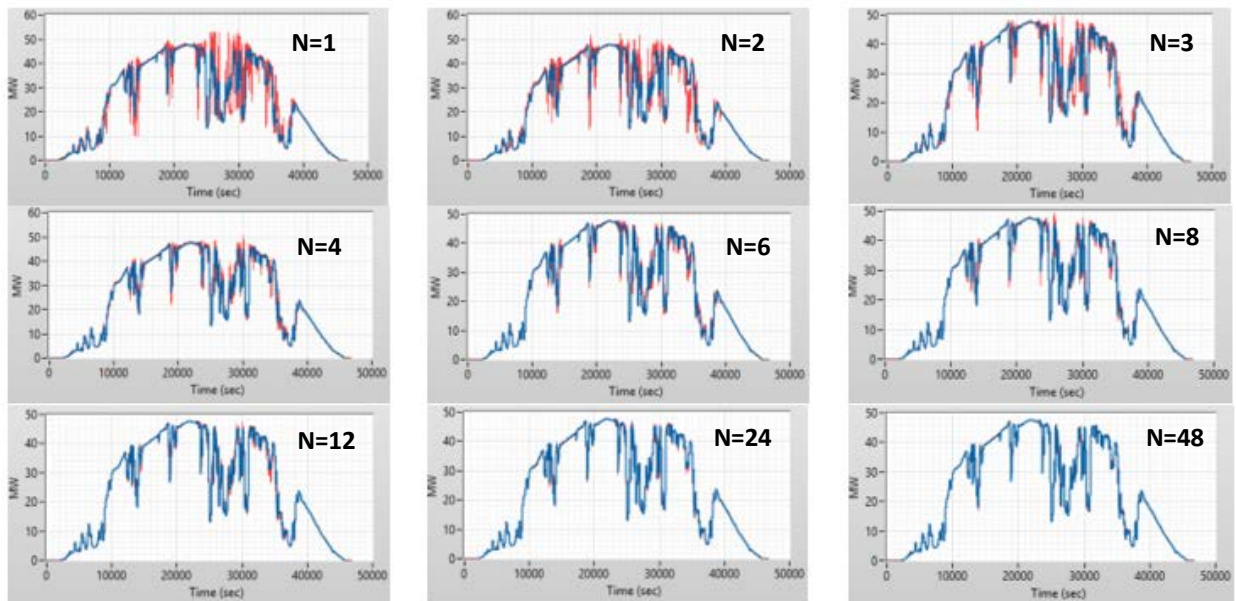


Figure 14. Improving measured total plant power when operating in MPPT mode; red: estimated total plant power for different numbers of reference inverters.)

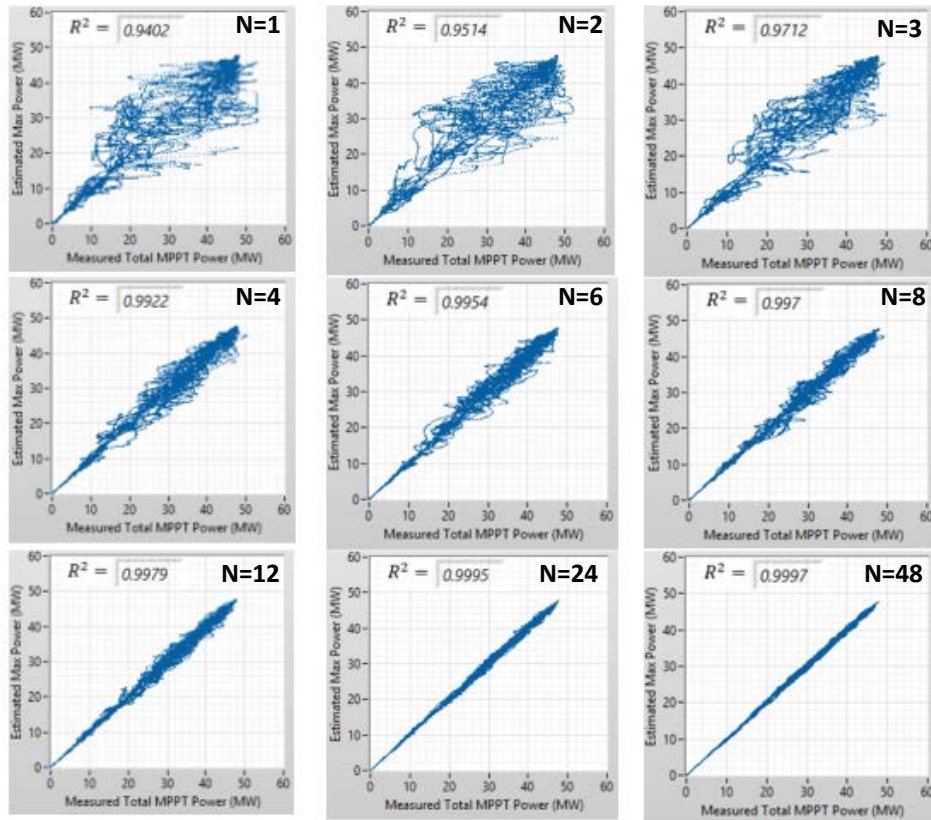


Figure 15. Improving the correlation between measured and evaluated maximum power by using a larger number of reference inverters: intense variability case

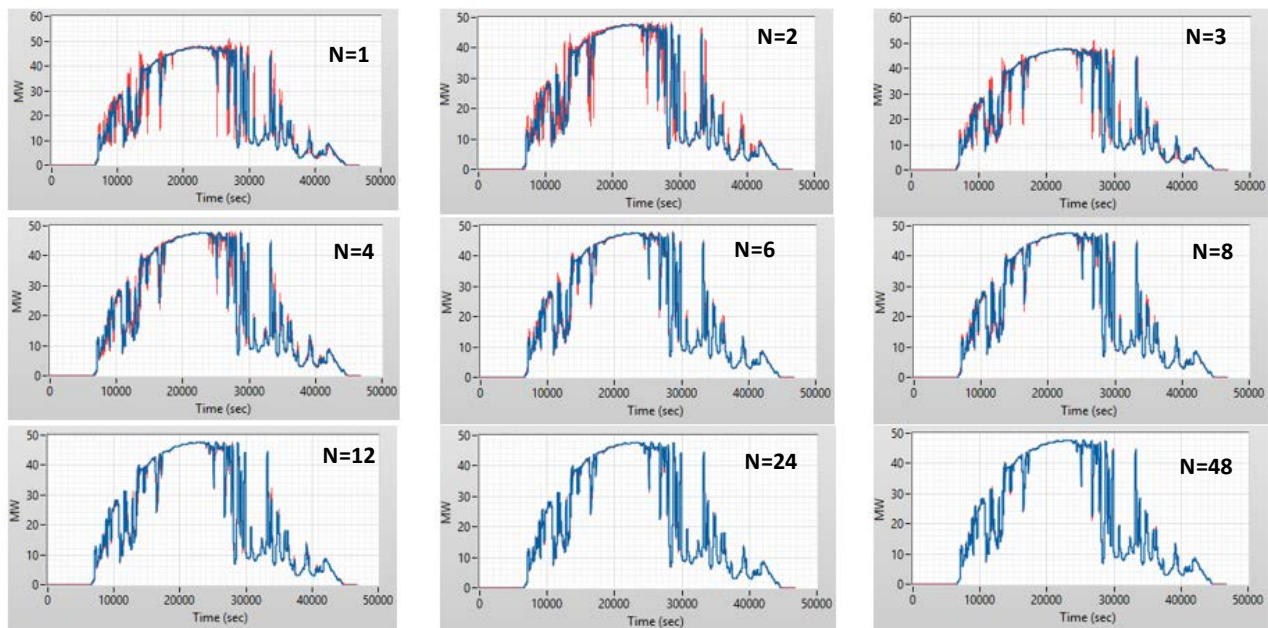


Figure 16. Improving the accuracy of maximum power evaluation by using a larger number of reference inverters: extreme variability case. (Blue: measured total plant power when operating in MPPT mode; red: estimated total plant power for different numbers of reference inverters.)

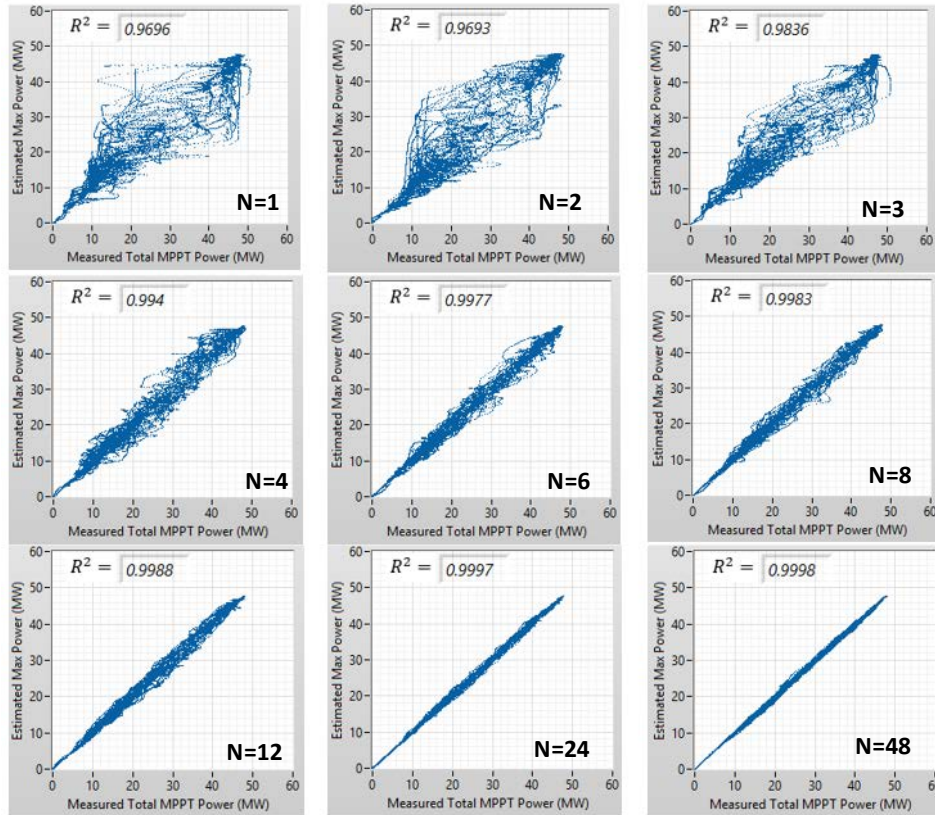


Figure 17. Improving the correlation between measured and evaluated maximum power by using a larger number of reference inverters: extreme variability case

Calculations performed for three variability cases (moderate, intense, and extreme) demonstrated continuous improvements in the accuracy of estimated maximum PV plant power. This can be observed from both 1-s time series graphs and 1-s correlation X-Y charts for the moderate variability case (Figure 12 and Figure 13), intense variability case (Figure 14 and Figure 15), and extreme variability case (Figure 16 and Figure 17), respectively. For all three cases, the best correlation is achieved with the largest number of reference MPPT inverters. This is explained by the varying nature of solar irradiance across the plant footprint, causing the diversity in the output power level between individual inverters. Therefore, having a larger number of dedicated reference MPPT inverters scattered all over the PV power plant would help achieve better accuracy in peak power estimation. Figure 18 demonstrates this fact at a higher resolution for the extreme variability case. This 10-min snapshot shows how the increasing numbers of reference inverters help improve the maximum power evaluation accuracy under varying conditions.

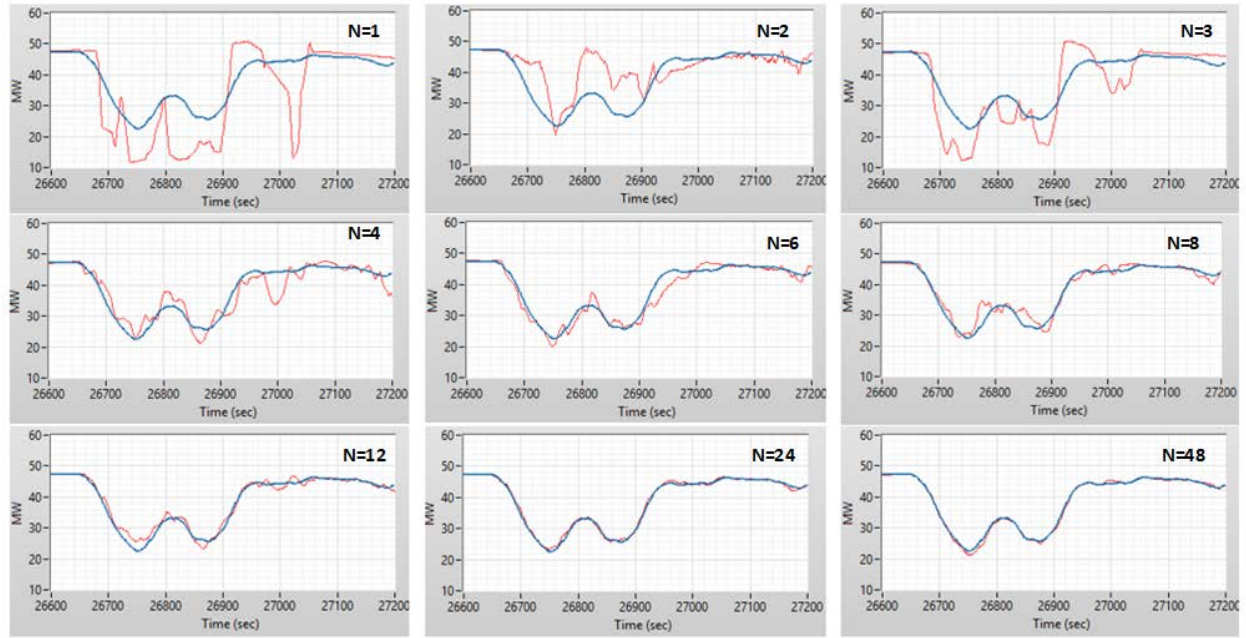


Figure 18. Improving accuracy for an extreme variability case. (Blue: measured total plant power when operating in MPPT mode; red: estimated total plant power for different numbers of reference inverters)

6 Maximum Power Estimation Error Statistics

Figure 19A and Figure 18B show the frequency distribution of error in estimating the maximum available PV plant power for different numbers of reference inverters in the moderate and extreme variability cases, respectively. These distributions were calculated for a large number of bins and are shown in logarithmic scale as a visual representation of the difference in the estimation error between the number of inverters and the large range of values. These distribution shapes are concentrated in the center, with large visible tails for fewer numbers of reference inverters. The distribution tails drop significantly with increasing numbers of reference inverters, achieving essentially a no-tail distribution when $N = 24$ or 48 for both the moderate and extreme variability cases.

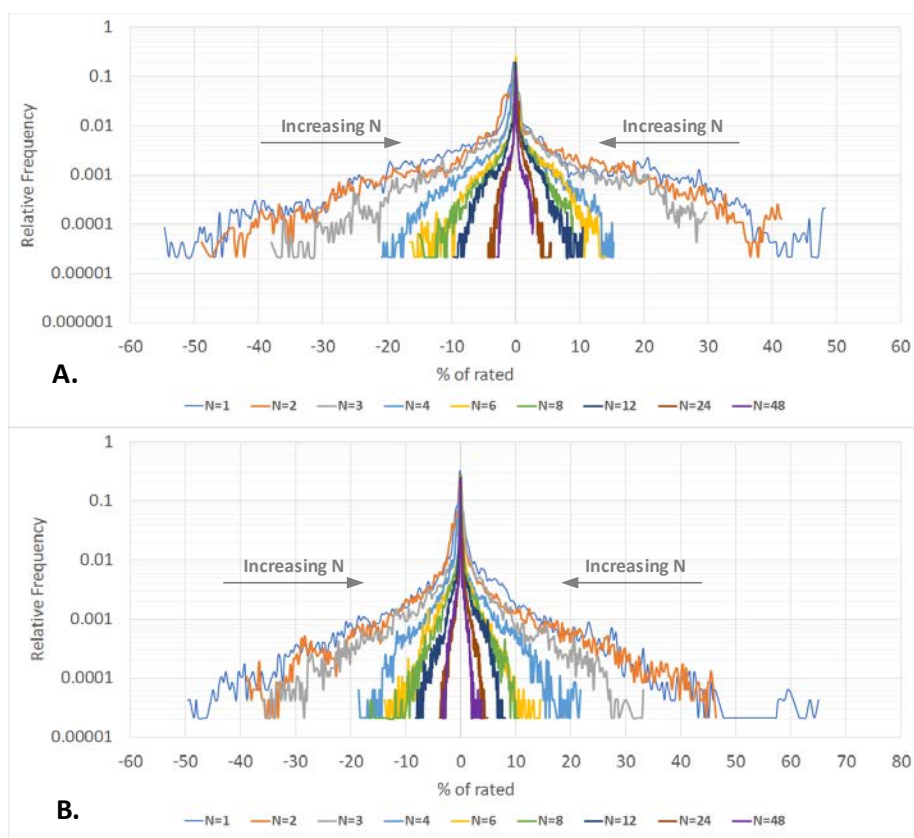


Figure 19. Reduction of control error with increasing numbers of reference inverters. (A: moderate variability case; B: extreme variability case.)

Table 1–Table 4 list the average, standard deviation, and min/max available plant power estimation errors, respectively, for all four variability cases as a percentage of plant rated power. The average (or mean) values and standard deviation of the error distributions are changing with the number of reference inverters, reaching insignificant levels with larger numbers of reference inverters. Similarly, the largest 1-s positive and negative peak power estimation errors reduce significantly with increased numbers of reference inverters. For example, in the extreme variability case, the maximum positive evaluation error was reduced from 50.5% ($N=1$) to 7.9% ($N=48$) of rated plant power, and the maximum negative evaluation error was reduced from -55.8% ($N=1$) to -9.2% ($N=48$) of rated plant power.

Skewness is a measure of symmetry. Table 5 shows that the distribution of errors is not exactly symmetric, with larger numbers of positive or negative tails, depending on the variability case and number of reference inverters. This means that particular periods of data collection sometimes produced larger numbers of positive 1-s errors than negative errors, and vice versa, depending on the variability conditions and number of reference inverters used in the estimation process.

Kurtosis is the measure of peakedness of distribution. Based on the kurtosis values in Table 6, it appears that the distribution of peak power estimation errors is relatively more peaked for higher variability cases. More-peaked distribution means that the higher frequency of smaller errors is concentrated around the central axes.

Table 1. Mean Peak Power Evaluation Error (% of Plant Rated Power)

N _{ref}	Clear Sky	Moderate Variability	Intense Variability	Extreme Variability
1	-1.572	-1.243	-1.411	-0.656
2	-1.325	-0.925	-1.242	-0.547
3	-1.034	-0.785	-1.084	-0.31
4	-0.984	-0.686	-1.039	-0.254
6	-0.703	-0.531	-0.894	-0.216
8	-0.643	-0.457	-0.652	-0.152
12	-0.39	-0.383	-0.443	-0.088
24	-0.129	-0.058	-0.281	-0.038
48	-0.035	-0.037	0.062	0.014

Table 2. Standard Deviation of Peak Power Evaluation Error (% of Plant Rated Power)

N _{ref}	Clear Sky	Moderate Variability	Intense Variability	Extreme Variability
1	0.939	6.437	8.180	6.275
2	0.735	6.190	7.525	5.934
3	0.546	5.605	6.877	5.267
4	0.527	5.296	6.417	5.081
6	0.361	4.601	5.668	4.656
8	0.326	3.831	5.317	3.976
12	0.192	2.472	3.019	3.481
24	0.091	1.817	2.386	2.106
48	0.070	0.977	1.408	1.156

Table 3. Maximum Positive Peak Power Evaluation Error (% of Plant Rated Power)

N _{ref}	Clear Sky	Moderate Variability	Intense Variability	Extreme Variability
1	3.329	58.729	45.800	50.566
2	2.091	54.389	43.859	47.678
3	1.213	55.146	42.003	45.254
4	1.183	45.527	41.808	45.408
6	0.564	34.479	39.957	39.582
8	0.494	28.121	33.959	28.893
12	0.315	15.270	19.935	22.891
24	0.2468	14.744	16.666	12.391
48	0.325	9.155	8.966	7.958

Table 4. Maximum Negative Peak Power Evaluation Error (% of Plant Rated Power)

N _{ref}	Clear Sky	Moderate Variability	Intense Variability	Extreme Variability
1	-3.635	-44.829	-52.92	-55.844
2	-3.210	-44.682	-45.702	-37.143
3	-2.289	-44.145	-46.761	-31.521
4	-2.177	-44.526	-38.979	-31.880
6	-1.654	-43.433	-28.235	-31.312
8	-1.461	-35.303	-27.046	-23.73
12	-0.916	-24.506	-17.528	-24.624
24	-0.482	-14.248	-12.806	-14.987
48	-0.256	-6.779	-7.777	-9.265

Table 5. Skewness of Peak Power Evaluation Error Distribution (% of Plant Rated Power)

N _{ref}	Clear Sky	Moderate Variability	Intense Variability	Extreme Variability
1	0.2495	2.085	-0.235	0.513
2	0.2185	1.755	-0.0213	0.562
3	0.2836	1.562	-0.212	0.555
4	0.2937	0.978	-0.005	0.740
6	0.305	-0.330	0.189	0.547
8	0.358	-0.376	0.136	0.241
12	0.373	-1.275	-0.182	-0.453
24	0.0244	1.0313	0.399	-0.644
48	1.264	0.377	0.571	-0.366

Table 6. Kurtosis of Peak Power Evaluation Error Distribution (% of Plant Rated Power)

N _{ref}	Clear Sky	Moderate Variability	Intense Variability	Extreme Variability
1	2.236	23.844	11.249	15.053
2	2.101	21.602	11.089	15.133
3	2.236	25.288	11.582	15.344
4	2.135	22.589	11.835	16.554
6	2.312	23.201	11.853	15.017
8	2.329	20.951	10.753	13.372
12	2.521	21.197	11.095	14.589
24	3.271	18.951	11.266	12.994
48	5.207	19.70	10.823	15.165

For a better visual perception of the data shown in Table 1–Table 6, we show the same data in graphical form to demonstrate the impact of increased numbers of reference inverters on improving the accuracy of the estimation statistics of the available power. Figure 20A and Figure 19B show reduction trends for mean estimation error and error standard deviation with increased numbers of reference inverters, respectively. Similarly, Figure 21A, Figure 20B, Figure 22A, and Figure 21B show improvements on min/max error and distribution skewness and kurtosis, respectively.

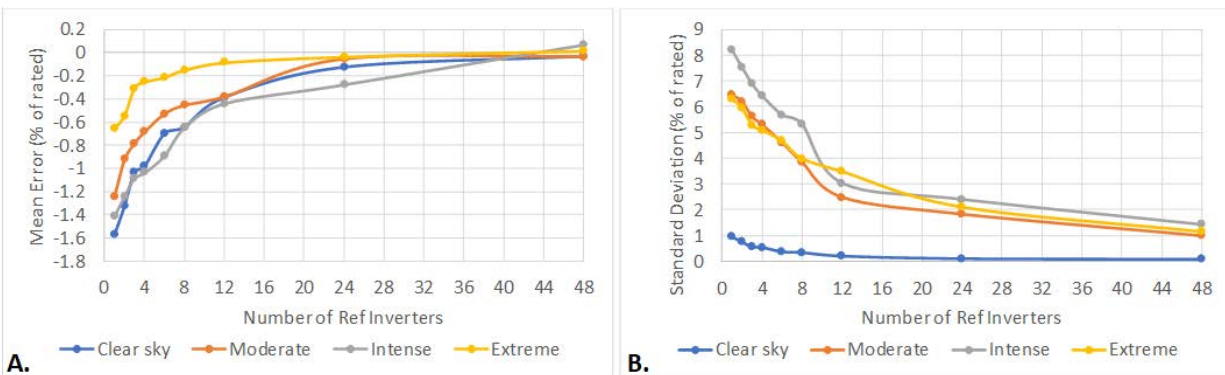


Figure 20. Mean error and standard deviation of error

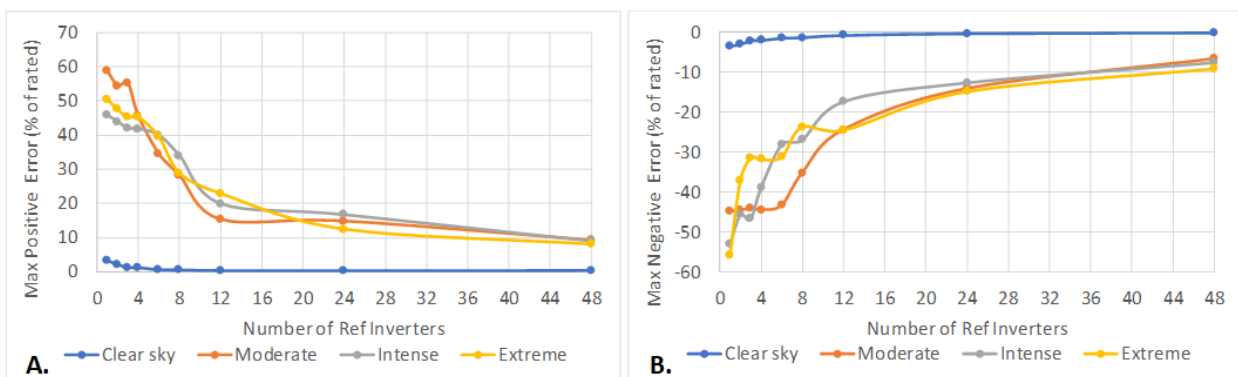


Figure 21. Min and max estimation error

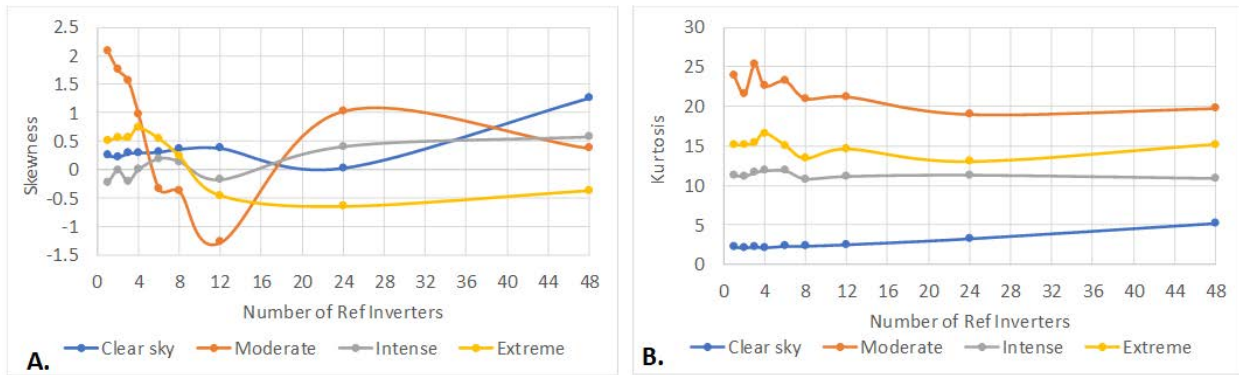


Figure 22. Skewness and kurtosis of error distribution

In addition, Table 7 shows how correlation coefficients between actual and estimated 1-s available power improve significantly with increasing numbers of reference inverters for all four variability conditions. The same data are consolidated and shown in Figure 23 as well.

Table 7. Correlation Coefficients Between Actual and Estimated Available Power for All Variability Cases

N_{ref}	Clear Sky	Moderate Variability	Intense Variability	Extreme Variability
1	0.995	0.979	0.947	0.947
2	0.998	0.983	0.955	0.947
3	0.999	0.987	0.963	0.956
4	0.999	0.988	0.968	0.959
6	0.999	0.990	0.974	0.967
8	0.999	0.992	0.976	0.977
12	0.999	0.994	0.992	0.990
24	1.000	0.998	0.995	0.995
48	1.000	0.999	0.998	0.998

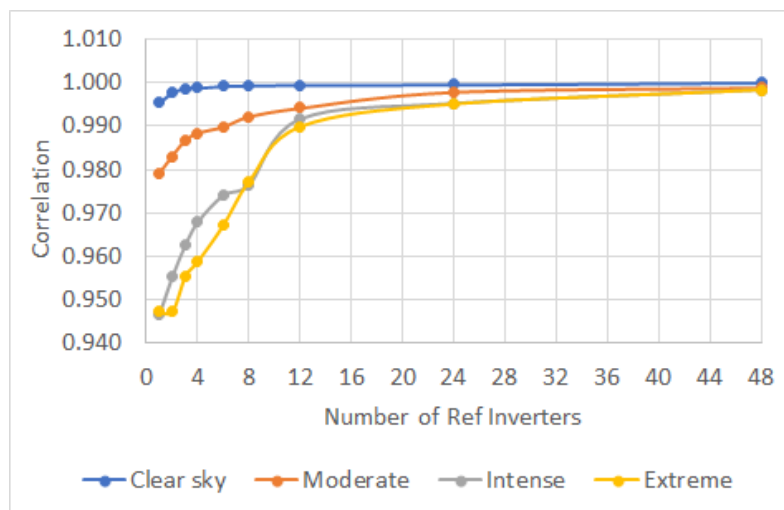


Figure 23. Correlation coefficients for all variability cases

7 Conclusions

In this report, we examined the peak power estimation method for curtailed PV power plants based on using dedicated reference inverters within a plant. The proposed technique does not require deploying any additional equipment or sensors and is based only on the addition of new control logic to the existing power plant controller. Based on our calculations using measured 1-s power production data from the entire PV power plant and individual inverters, the method has the potential to produce highly accurate real-time estimates of available aggregate peak power that all the plant's inverters can produce at any point in time and ensure that the control error stays within the desired tolerance bands at all times.

To complete the validation of the proposed PV plant peak power evaluation method, First Solar and the National Renewable Energy Laboratory are planning to conduct demonstration testing on a large utility-scale PV power plant installed at the National Wind Technology Center under a cooperative research-and-development collaboration. An aerial photo of the plant is shown in Figure 24. This PV plant is rated for 430 KWac and uses six PV string inverters. The architecture of the PPC for this PV plant allows for easy control modifications, so the proposed concept can be validated with real hardware under real resource variability conditions. The National Wind Technology Center test site offers unique testing conditions for this experiment because of the extreme solar resource variability conditions present at the site.



Figure 24. Aerial photo of First Solar PV plant at the National Renewable Energy Laboratory's National Wind Technology Center

8 Future Plans

Areas of future research include the development of optimized control strategies to achieve the minimum peak power estimation error under all types of operational scenarios for PV plants. Several optimization objectives must be resolved by the reserve allocation controller, which will dispatch reference inverters every predetermined time interval, ΔT (every 10 s, for example):

1. Determine the optimal number of control zones, N_{zones} , for the given variability conditions. (This could be determined from the forecast as well.)
2. Determine the optimal location of a reference inverter in each zone.
3. Determine the optimal dispatch interval, ΔT , for the reference MPPT inverters. (This will probably be longer for clear-sky days and shorter for highly variable days.)
4. Determine the optimized combinations of curtailment set points for participating inverters in each zone for maximum aggregate inverter efficiency (or minimum electric losses in the plant) for every ΔT interval. (Typical inverter efficiencies are shown in Figure 25.)
5. Use the short-term energy storage to correct estimation errors.

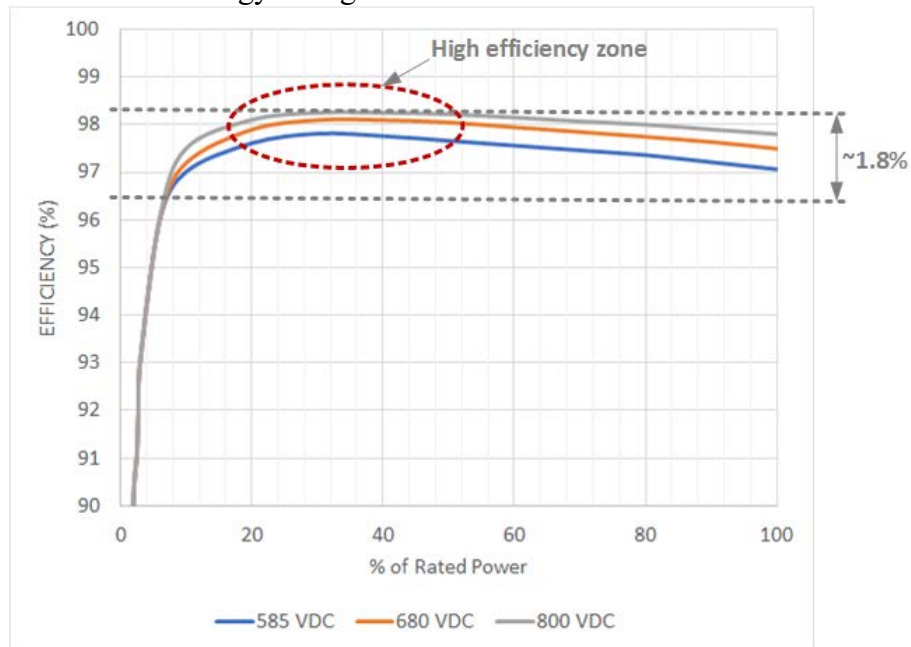


Figure 25. Typical MW-scale PV inverter efficiencies

References

- [1] C. Loutan, P. Klauer, S. Chowdhury, S. Hall, M. Morjaria, V. Chadliev, N. Milam, C. Milan, and V. Gevorgian, *Demonstration of Essential Reliability Services by a 300-MW Solar PV Plant* (NREL/TP-5D00-67799) (Golden, CO: National Renewable Energy Laboratory, March 2017).
- [2] Federal Energy Regulatory Commission, “Docket No. RM16-23-000: Electric Storage Participation in Markets Operated by Regional Transmission Organizations and Independent System Operators” (2016).
- [3] North American Electric Reliability Corporation, *Integration of Variable Generation Task Force Report* (Washington, D.C.: 2012).
- [4] North American Electric Reliability Corporation, *Essential Reliability Services Working Group and Distributed Energy Resources Task Force Measures* (Washington, D.C.: 2012).
- [5] ENTSO-E, “ENTSO-E Network Code for Requirements for Grid Connection Applicable to All Generators” (March 2013).
- [6] VDE, *Technical Requirements for the Connection to and Parallel Operation with Low-Voltage Distribution Networks* (VDE-AR-N 4105) (Frankfurt, Germany).
- [7] Federal Energy Regulatory Commission, “Order 842: Essential Reliability Services and the Evolving Bulk-Power System—Primary Frequency Response” (2018).
- [8] North American Electric Reliability Corporation, “BAL-003-1 Frequency Response and Frequency Bias Setting Standard” (2016).
- [9] California Independent System Operator, *CAISO 5th Replacement Electronic Tariff, Appendix A: Master Definition Supplement* (Folsom, CA: February 1, 2017).
- [10] A. Hoke, E. Muljadi, and D. Maksimovic, “Real-Time Photovoltaic Plant Maximum Power Point Estimation for Use in Grid Frequency Stabilization,” presented at the 2015 IEEE Workshop on Control and Modeling for Power Electronics.
- [11] E. Batzelis, G. Kampitsis, and S. Papathanassiou, “Power Reserves Control for PV Systems with Real-time MPP Estimation via Curve Fitting,” *IEEE Transactions on Sustainable Energy* 8, no. 3 (July 2017).
- [12] T. Hiyama and K. Kitabayashi, “Neural Network-Based Estimation of Maximum Power Generation from PV Module Using Environmental Information,” *IEEE Transactions on Energy Conversion* 12, no. 3 (1997): 241–247.
- [13] M. Taherbaneh and K. Faez, “Maximum Power Point Estimation for Photovoltaic Systems Using Neural Networks,” *Proceedings of the 2007 IEEE International Conference on Control and Automation* (2007: 1614–1619).
- [14] J.-C. Wang, Y.-L. Su, J.-C. Shieh, and J.-A. Jiang, “High-Accuracy Maximum Power Point Estimation for Photovoltaic Arrays,” *Solar Energy Materials and Solar Cells* 95, no. 3 (2011): 843–851.
- [15] A. Garrigós, J.M. Blanes, J.A. Carrasco, and J.B. Ejea, “Real Time Estimation of Photovoltaic Modules Characteristics and Its Application to Maximum Power Point Operation,” *Renewable Energy* 32, no. 6 (2007): 1059–1076.
- [16] J. Ma, K.L. Man, T.O. Ting, N. Zhang, S.-U. Guan, and P.W. Wong, “Dem: Direct Estimation Method for Photovoltaic Maximum Power Point Tracking,” *Procedia Computer Science* 17 (2013): 537–544.
- [17] G. Kumar and A.K. Panchal, “Geometrical Prediction of Maximum Power Point for Photovoltaics,” *Applied Energy* 119 (2014): 237–245.

- [18] Y. Liu, L. Chen, L. Chen, H. Xin, and D. Gan, “A Newton Quadratic Interpolation Based Control Strategy for Photovoltaic System,” in *Proceedings of the 2012 International Conference on Sustainable Power Generation and Supply* (Hangzhou, China: September 2012, Paper.611 CP).
- [19] B.-I. Craciun, T. Kerekes, D. Sera, and R. Teodorescu, “Frequency Support Functions in Large PV Power Plants with Active Power Reserves,” *IEEE Journal of Emerging and Selected Topics in Power Electronics* 2, no. 4 (2014): 849–858.
- [20] V.A.K. Pappu, B. Chowdhury, and R. Bhatt, “Implementing Frequency Regulation Capability in a Solar Photovoltaic Power Plant,” in *Proceedings of the 2010 North Amer. Power Symposium* (Arlington, TX: September 2010, Art. no.5618965)
- [21] S. Shedd, B.-M. Hodge, A. Florita, and K. Orwig, “A Statistical Characterization of Solar Photovoltaic Power Variability at Small Timescales,” presented at the 2nd Annual International Workshop on Integration of Solar Power in Power Systems Conference, Lisbon, Portugal, November 12–13, 2012.
- [22] V. Gevorgian, and B. O’Neill, *Advanced Grid-Friendly Controls Demonstration Project for Utility-Scale PV Power Plants* (NREL/TP-5D00-65368) (Golden, CO: January 2016).
- [23] G. Box, G. Jenkins, and G. Reinsel, *Time Series Analysis* (ISBN 0-13-060774-6) (Upper Saddle River, NJ: Prentice-Hall, 1994).
- [24] E.J. Gumbel, *Statistics of Extremes* (ISBN 0-486-43604-7) (New York: Columbia University Press, 1998).
- [25] “The R Project for Statistical Computing: The R Manuals.” Online resource. www.rproject.org.
- [26] D.W. Scott. “On Optimal and Data-Based Histograms,” *Biometrika* 66, no. 3 (1979): 605–610.